INSTITUTE OF PLASMA PHYSICS
CZECHOSLOVAK ACADEMY OF SCIENCES

VELOCITY SPREAD OF REB GENERATED BY HIGH CURRENT DIODE

P. Vrba

RESEARCH REPORT

IPPCZ - 339

May 1994

POD VODÁRENSKOU VĚŽÍ 4, 180 69 PRAGUE 8
CZECHOSLOVAKIA

VELOCITY SPREAD OF REB GENERATED BY HIGH CURRENT DIODE

P. Vrba

IPPCZ-339 May 1994

VELOCITY SPREAD OF REB GENERATED BY HIGH CURRENT DIODE

Institute of Plasma Physics, Acad. Sci. of Czech Rep., Za Slovankou 3, 180 69 Prague 8, Czech Republic

P. Vrba

March 25, 1994

Abstract

Theoretical analysis and numerical simulations of Relativistic Electron Beam (REB) generation in high current diode immersed in external magnetic field has been done. The calculations confirmed that the generated beam is homo- geneous and monoenergetic in a broad central region. In the case of cylindrical diode the mixing of electron trajectories has been only observed in a narrow periphery beam region. The angle between particle trajectories and external longitudinal magnetic field varies chaotically from 0^0 to -25^0. This phenomenon suppresses the excitation of two stream instability excited by REB in the plasma column. [illegible]

1 INTRODUCTION

For various applications, including plasma heating in a long solenoid, the homogeneous and monoenergetic REB is necessary. Usually, the high current diode with strong guiding magnetic field is used. Besides the beam homogeneity the important characteristic is angular velocity spread of particles leaving vacuum diode. This angular velocity spread strongly affects the the beam-plasma interaction in the plasma heating experiment.

When the REB is injected into the plasma column kinetic or hydrodynamic mode of two stream instability can be excited. The transition from kinetic to hydrodynamic mode occurs if the initial scattering angle θ, characterizing the beam angular velocity spread [1], satisfies the following condition $\bar{\theta}^2 \simeq \frac{2^{4/3}}{\sqrt{3}}\eta^{2/3}$, where $\eta \equiv \frac{n_b}{n_p}$ is the beam and plasma density ratio. The REB with smaller angular

velocity spread can excite the hydrodynamic mode instability in the plasma with higher density.

We present here a detailed numerical study of the beam generation in cylindrical diodes under the presence of strong external magnetic field to understand the angular velocity spread observed in our experiments [2]. In our two dimensional description the angular velocity spread is described by the incident angle c, which is defined as the angle between particle trajectories projection and external magnetic field. For our REB ($E_b = 350\ keV$, $I_b \simeq 45\ kA$) the hydrodynamic mode of two stream instability is expected in plasma column ($\frac{n_b}{n_p} \simeq \frac{2}{3}.10^{-3}$) if the incident angle $c < 7^0$. The aim of our simulation is further optimization of high current diodes with small angular spread.

2 THEORETICAL ESTIMATION

2.1 The Influence of Cathode Shape on Diode Current

For generation of REB high current diodes with the high aspect ratio $\frac{R}{d_0} \gg 1$ (where R is diode radius and d_0 is diode gap) are used. The cathode - anode distance d(r) is smooth increasing function of cylindrical coordinate r. Under these circumstances the total current I through the diode is [3]

$$I = I_0 . \max_r [\frac{r}{d(r)}] . \min_x F(\gamma, x)$$

where $I_0 \equiv \frac{mc^3}{2e}$ (in Gaussian units). In SI units, $I_0 \doteq 8500\ A$.

The maximum of the function $\frac{r}{d(r)}$ for different cathode shape are determined in Appendix I.

The function

$$F(\gamma, x) \equiv \frac{\gamma - \frac{1}{x}}{\sqrt{1 - v^2}} + \frac{1}{v} ln(\frac{1}{x} + \sqrt{\frac{1}{x^2} - 1})$$

depends on relativistic factor $\gamma = \frac{1}{\sqrt{1-\beta^2}}$, $\beta = \frac{v}{c}$. The current ratio $x = \frac{I_c(r)}{I}$, where I_c is the current emitted by the inner part of cathode surface within the radius r to the total current flowing through the diode. We overtake the value of function $\min_x F(\gamma, x)$ in graphical form (see Fig. 1) from the work [3].

2.2 The Diode Immersed into Strong Magnetic Field

The boundary effects on diode periphery are suppressed by the application of strong external longitudinal magnetic field B_0. Under certain circumstances, the beam current in cylindrical diode is equivalent to the current in ideal planar diode. If the external longitudinal magnetic field is sufficiently high the electrons gyrate

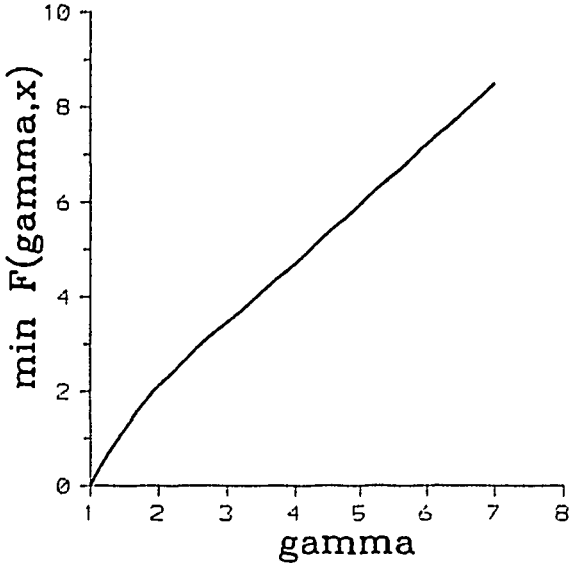

Figure 1: The minimum of the function F(γ,x)

around and move along the magnetic field lines. The longitudinal part of electron velocity is

$$v_z = \frac{v}{[1 + (\frac{b_\varphi}{B_0})^2]^{1/2}}$$

where $\frac{b_\varphi}{B_0}$ is magnetic (internal to external) field ratio, for the total velocity we have $v = c[1 - (1 + \frac{e\varphi}{mc^2})^{-2}]^{1/2}$.

The potential φ is determined by solving Poisson eq.

$$\frac{\partial^2 \varphi}{\partial z^2} = 4\pi e n_e$$

where n_e is the electron beam density. Poisson eq. is solved with the following boundary conditions: on the cathode $\varphi\,|_{z=0} = 0$, $\frac{\partial \varphi}{\partial z}\,|_{z=0} = 0$ and on the anode $\varphi\,|_{z=d} = \frac{mc^2}{e}(\gamma - 1)$.

The azimuthal component of internal magnetic field follows from Biot-Savart law

$$\frac{\partial b_\varphi}{\partial z} = \frac{4\pi}{c} e n_e v_r$$

where v_r is radial beam velocity component.

From the solution of above mentioned equations the longitudinal current beam density

$$j_z \equiv -e n_e v_z = -j_0 \frac{g(\gamma)}{[1 + (\frac{b_\varphi}{B_0})^2]^{1/2}}$$

where $j_0 \equiv \frac{mc^3}{2\pi e d^2}$ (in Gassian units) is obtained. The function

$$g(\gamma) \equiv \frac{1}{4}[\int_1^\gamma \frac{dx}{(x^2 - 1)^{1/4}}]^2$$

Table 1: THE MEASURABLE PLANAR DIODE PARAMETERS

ξ	r	$\frac{v_z}{v}$	ϵ	j_z
	mm		deg	MA/m^2
0.00	0.0	1.000	$+00^0\ 00'$	66.3
0.25	3.6	0.992	$-07^0\ 07'$	65.8
0.50	7.2	0.970	$-14^0\ 02'$	64.3
0.75	10.8	0.945	$-19^0\ 09'$	62.8
1.00	14.4	0.917	$-23^0\ 33'$	60.8
1.25	18.0	0.884	$-27^0\ 50'$	58.6
1.50	21.6	0.846	$-32^0\ 11'$	56.1

depends on relativistic factor γ (see [3]), and for our case of relativistic beam accelerated up to energy $E_b = 400\ keV$ ($\gamma \doteq 1.8$) the value of $g(1.8) \doteq 0.22$.

The trajectories of relativistic electrons are curved, the incident angle on anode foil is $\epsilon = -arccos(\frac{v_z}{v})$. The value of the quantity $\frac{v_z}{v}$ and beam current density j_z depends on beam radius r (normalized variable $\xi \equiv \frac{r}{d}\frac{2mc^2}{edB_0}g(\gamma)$ are summarized in Tab. 1. The following diode parameters were taken into account; gap dimension $d_0 = 3\ mm$, the value of external magnetic field $B_0 = 12\ kG$ and the electron beam energy $E_b = 400\ keV$. The above mentioned expressions are valid when the value of external magnetic field $B_0 \gg B_c = \frac{mc^2}{eR}\frac{(\gamma-1)^2}{g(\gamma)} \doteq 1\ kG$, hence the approximation is acceptable.

The total beam current of plane diode with the radius R and slot dimension d_0 immersed in external longitudinal magnetic field is determined by

$$I = \frac{RcB_0}{2}h(\xi_0)$$

where $\xi_0 = \frac{R}{d}\frac{2mc^2}{edB_0}g(\gamma)$. In our case, when $R = 2\ cm$, $d = 0.3\ cm$, $B_0 = 12\ kG$ and $\gamma \doteq 1.8$ the value of normalized variable $\xi_0 \doteq 1.388$, $h(\xi_0) \doteq 0.635$ and the value of total diode current $I \simeq 76.2\ kA$.

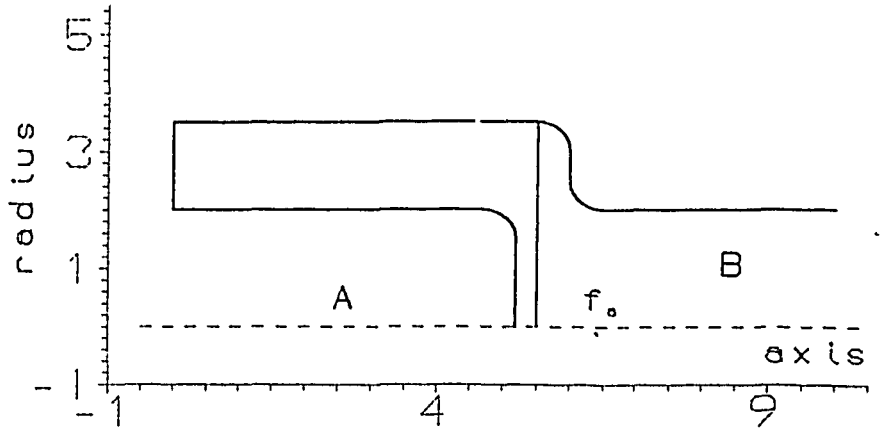

Figure 2: Scheme of cylindrical diode

A - diode region, B - plasma column,
f_a - anode foil.

3 THE REB SIMULATION IN HIGH CURRENT DIODE

3.1 The Steady State

The two-dimensional relativistic electro-magnetic current line code 'POISSON2' [4] is used to simulate the forming of stationary REB in high current diode.

The diode parameters and performance values are summarized in Tab. 2. Two different regions are seen on Fig. 2 inside the diode volume:

A - evacuated cathode-anode diode region where the high current REB is generated,

B - plasma column through which propagates the electron beam. In this region the beam energy is deposited into the plasma via excited two stream instability. The evacuated part of the diode is separated from anode plasma column by thin foil f_a.

The multiple spatial grid was used, there were three zones in radial direction ($KZONR = 3$) and three zones in longitudinal direction ($KZONZ = 3$). Fine rectangular meshes ($\Delta r = \Delta z = 0.5\ mm$) were used on the periphery of generated REB near the anode surface. The total number of mesh points was equal to $40x42 = 1680$.

At the very beginning of the diode performance the electrons were emitted by three fronts ($KFR = 3$) covering central, edge and cylindrical part of cathode surface. The electron beam was described by $30 + 40 + 20 = 90$ tubes. The tube

Table 2: DIODE parameters.

A - diode region	(cm)
cathode length l_c	5.2
cathode-anode spacing d_0	0.3
cathode radius r_c	2.0
anode radius r_a	3.5
cathode edge radius r_{ed}	0.5
cathode voltage V_{cat} (MV)	-0.40
magnetic field B_0 (T)	1.2
B - anode plasma column	
plasma column length L_{pl}	5.50
plasma column radius R_{pl}	2.75
edge radii r_1, r_2	0.5
foil thickness t_a	0.001

widths were comparable with mesh grids. The minimum width $l_{tb} \sim 0.2\ mm < \Delta r \simeq \Delta z$ had tubes emitted by edge cathode part. The starting value of the emission current density correlated with the Child Langmuir law ($TIP = 1$).

The relaxation procedure describing how to obtain the steady state values of charge and currents densities on selected grid (potential, electric field and internal magnetic field intensity) was fully described in previous work [5].

The steady state relativistic electron flow was achieved after 18 relaxation steps (see Fig. 3), with the relaxation coefficient $\Omega = -0.075$. The value of the diode current was $I_b \simeq 76\ kA$. The central (edge) part of the beam carried $\simeq 56\%$ ($\simeq 42\%$) of the total current. Small portion ($\simeq 2\%$) was emitted by cylindrical diode part, where the electron emission was suppressed by the charge cumulated near the cathode surface. Some electrons were reflected back and traveled along the cathode (the similar case was described in the work [6]). The dependence of current emission density J_c on surface position s confirmed this phenomenon (see Fig.4). The value of current emission density was constant $J_c = 60\ MA/m^2$ for central diode part $0 \leq s \leq 15\ mm$. For the edge cathode part ($15\ mm \leq s \leq 22.8\ mm$) diminished to $J_c \doteq 10\ MA/m^2$. In the next small part $22.8\ mm \leq s \leq 25.5\ mm$ of third emission front fell $J_c \to 0$.

The map of equipotentials in cylindrical diode are seen on Fig.5. The equipotentials in central flat part followed the cathode surface. The potential φ grew up from the value $\varphi = -400\ kV$ on the cathode surface to $\varphi = 0\ kV$ on anode surface. The equipotentials continued around the cathode edge into cylindrical diode part. In central part of cylindrical region some equipotential points were shifted outside cathode surface. This shift was caused by the charge of emitted electrons which were unable to get on anode surface.

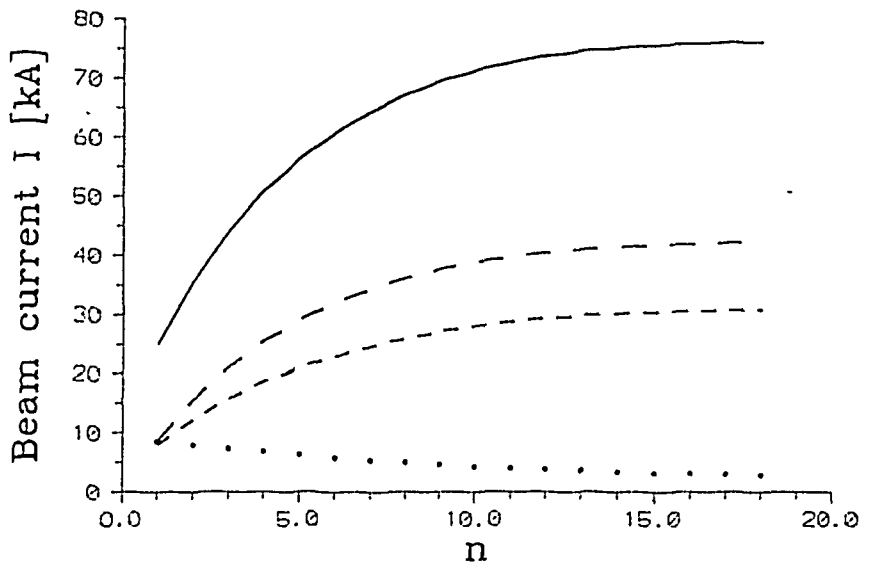

Figure 3: The relaxation of electron beam current to the steady state

$I_b = I_{central} + I_{edge} + I_{cylindrical}$ (full line), $I_{central}$ (dashed line), I_{edge} (short dashed line), $I_{cylindrical}$ (dotted line),
n - is number of relaxations steps.

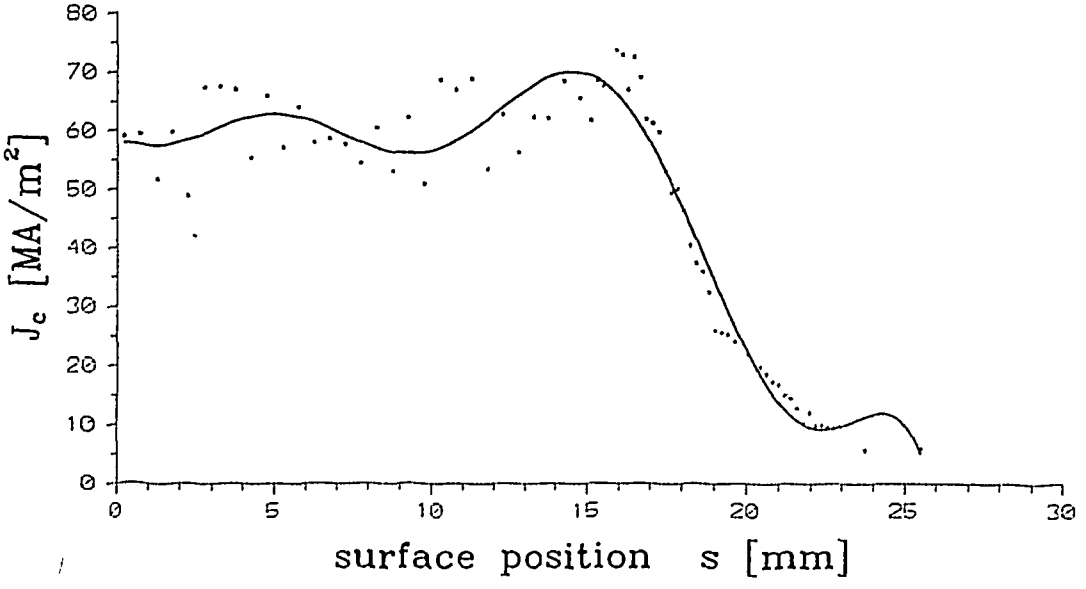

Figure 4: The dependence of beam current density J_c on surface position s

surface position s is measured from the centre of plane part of cylindrical diode

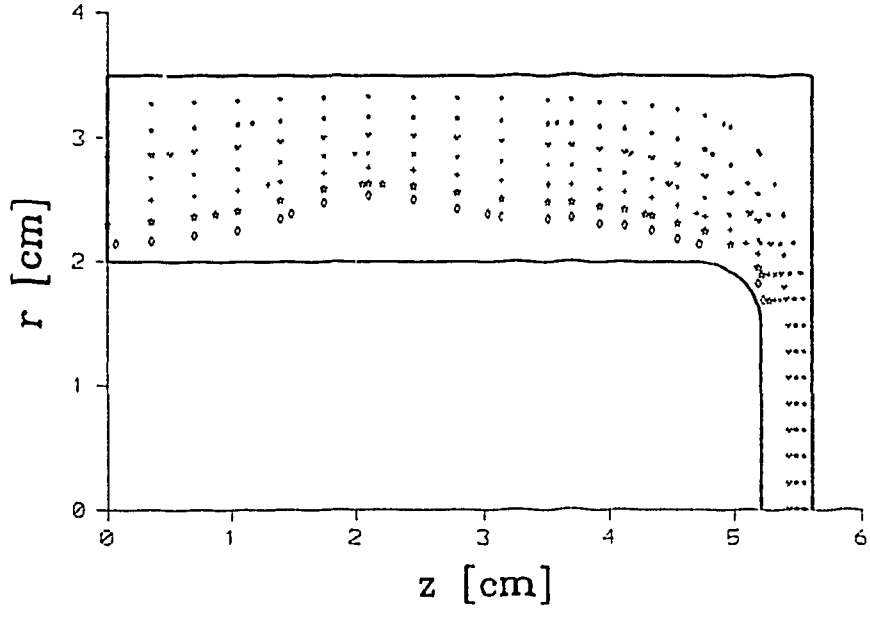

Figure 5: The map of equipotentials

$* = -50\ kV$, $\star = -100\ kV$, $\times = -150\ kV$, $\times = -200\ kV$, $+ = -250\ kV$, $\star = -300\ kV$, $\diamond = -350\ kV$

The map of electric field intensity lines, $E = \sqrt{E_r^2 + E_z^2} = E_{const}$, are seen on Fig. 6. The value of field intensity grew up from $E = 20\ kV/m$ on anode surface to the value of $E \geq 160\ kV/m$ near the cathode surface. The field lines followed the electrode surface and were successively ended on the cathode edge. Near the central cylindrical diode part ($1.38\ mm \leq z \leq 2.76\ mm$) the line $E = 40\ kV/m$ (marked by $\star$ on Fig. 6) created close area. In this region the emitted electrons were caught and oscillate forward and back along the cathode surface.

The azimuthal component of internal magnetic field b_φ is depicted for the end part of the cylindrical diode on Fig. 7. The field intensity grew up linearly with the beam radius in the range $0\ cm \leq r \leq r_c$. The maximum value of field intensity $b_\varphi^{max} \doteq 7.2\ kG$ was achieved at $r = r_c = 2\ cm$. The value of magnetic field ratio ($\frac{b_\varphi}{B_0} \simeq 0.6$) was rather high here. On the contrary of line conductor the azimuthal magnetic field was continuous at $r = r_c$. In the region outside the beam $r_c < r$ fell down inverse proportional to the coordinate r.

3.2 The Beam Properties on Anode Surface

Electrons, emitted from the cathode surface, accelerated by electric field, curved by external or internal magnetic fields, fall on different places of anode surface. The tube currents I_a transmitted through the diode are seen on Fig.8.

The dependence of beam current density J_a on the beam radius was determined (see Fig.9). During the calculation the different tube widths ($l_{tb} \simeq 0.5\ mm$ for

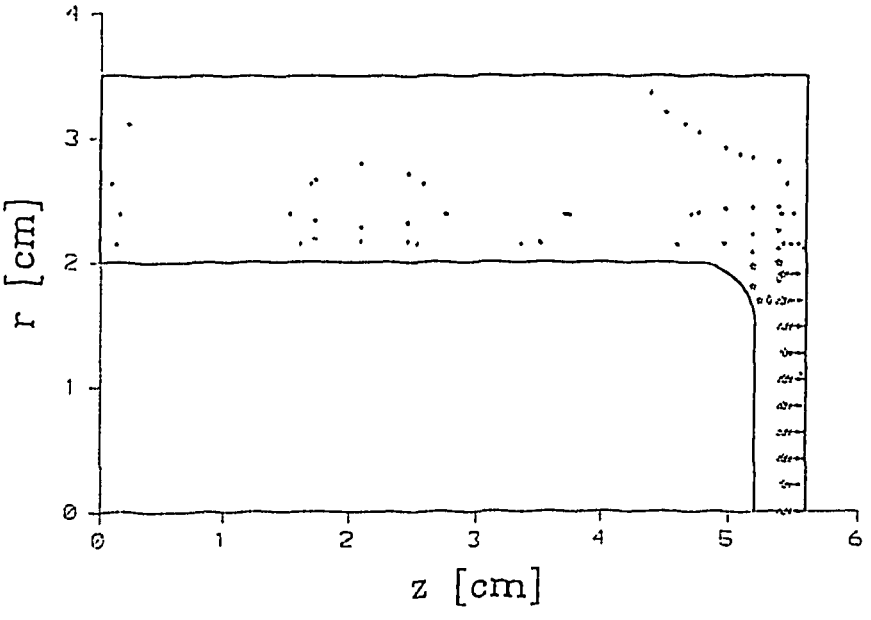

Figure 6: The map of electric field intensity lines

$* = 2.10^4\ V/m^2$, $* = 4.10^4\ V/m^2$, $\times = 6.10^1\ V/m^2$, $+ = 8.10^4\ V/m^2$,
$* = 1.10^5\ V/m^2$, $\diamond = 1.2.10^5\ V/m^2$, $\triangle = 1.4.10^5\ V/m^2$

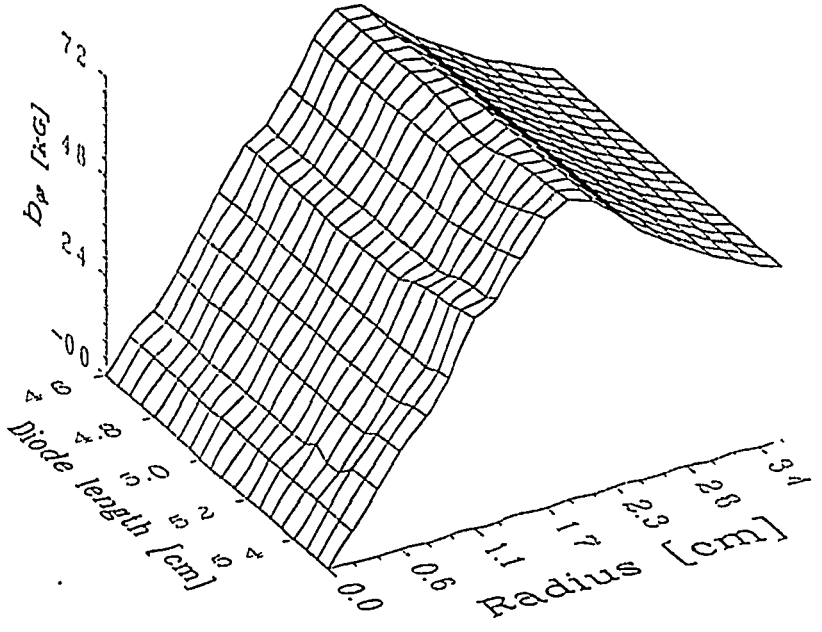

Figure 7: The azimuthal component b_φ of internal magnetic field

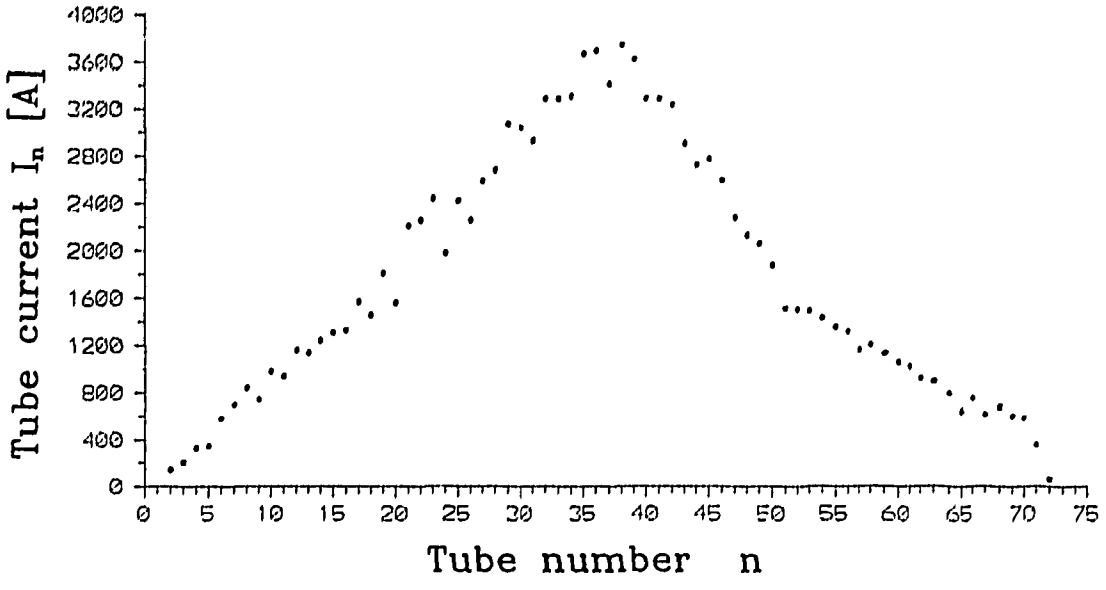

Figure 8: The dependence of tube current I_n on sequential tube number n

first front, $l_{tb} \simeq 0.2\ mm$ for second front and $l_{tb} \simeq 1.8\ mm$ for third emission front) and different tube positions on anode surface were taken into account. The nearly homogeneous REB, with the current beam density $j_z \simeq 70\ MA/m^2$, was generated in the region $0 \geq r \geq 1.8\ cm$). The current beam density fell to zero at $r > 2\ cm$.

The beam particles struck the anode foil under the incident angle $\epsilon \equiv arctg(\frac{v_r}{v_z})$. The dependence of incident angle $\epsilon(n)$ on the sequential tube number n is seen on the Fig. 10. The absolute value of incident angle grew up linearly with tube number in central diode part (for $1 \leq n \leq 42$). After that the absolute value of incident angle fell down (for $43 \leq n \leq 54$). For remaining tubes ($n \geq 55$) the values of incident angle changed chaotically. This phenomenon is evidently seen on the Fig. 11, where the dependence of incident angle $\epsilon(r)$ on beam radius is depicted. The value of incident angle linearly decreased ($\epsilon < 0^0$) with the increasing beam radius (see also [7]). For the last tube ($n = 30$) of first emission front, the incident angle was $\epsilon = -17^0\ 20'$ and the crossing point lay at $r = 14.04\ mm$ from the centre of the beam. The maximum departure of particle trajectory from longitudinal direction was achieved for the tube $n = 42$ and the crossing point lay at the distance $r = 16.6\ mm$. The particle with the incident angle $\epsilon = -2^0\ 30'$ moved along the diode axis and struck the anode surface at the distance $r = 18.6\ mm$. The trajectories mixing occurred for periphery beam part $r \geq 18.62\ mm$. Approximately $\frac{1}{10}$ of the total beam current flew in this narrow periphery beam part ($\Delta r_{per} \doteq 1.32\ mm$). The incident angle ϵ chaotically changed its value from -2^0 to -23^0 in this region. This phenomenon achieved by the simulation was not predicted by the theory.

The deflection of particle trajectories from magnetic field lines can partially be eliminated using specially designed coil. This elimination is practically impossible

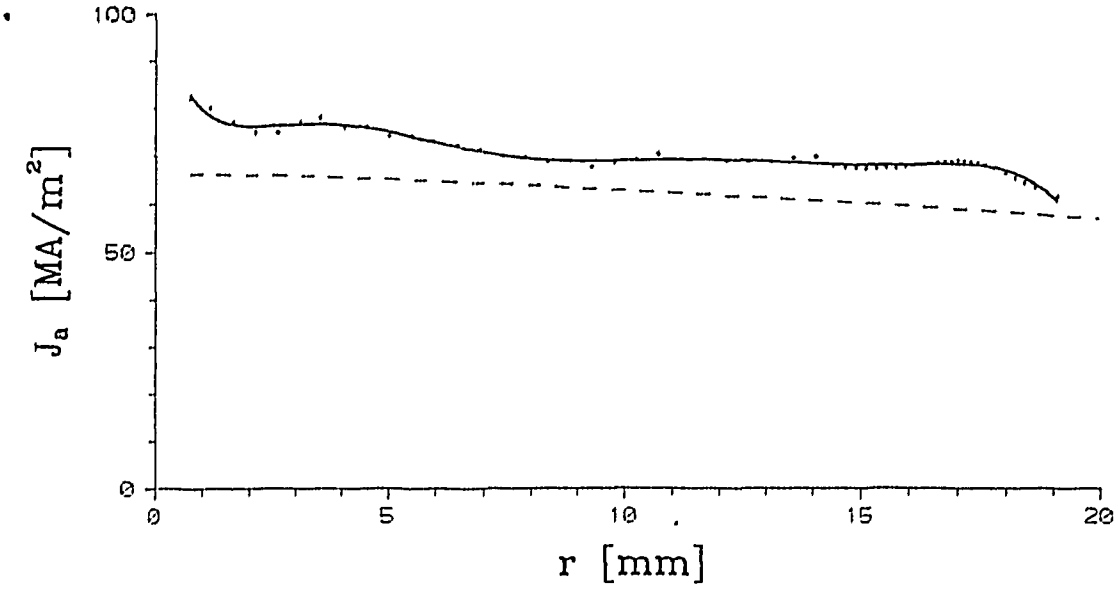

Figure 9: The radial dependence of the beam current density J_a

numerical simulation of cylindrical diode (solid line), theoretical calculation of planar diode (dashed line)

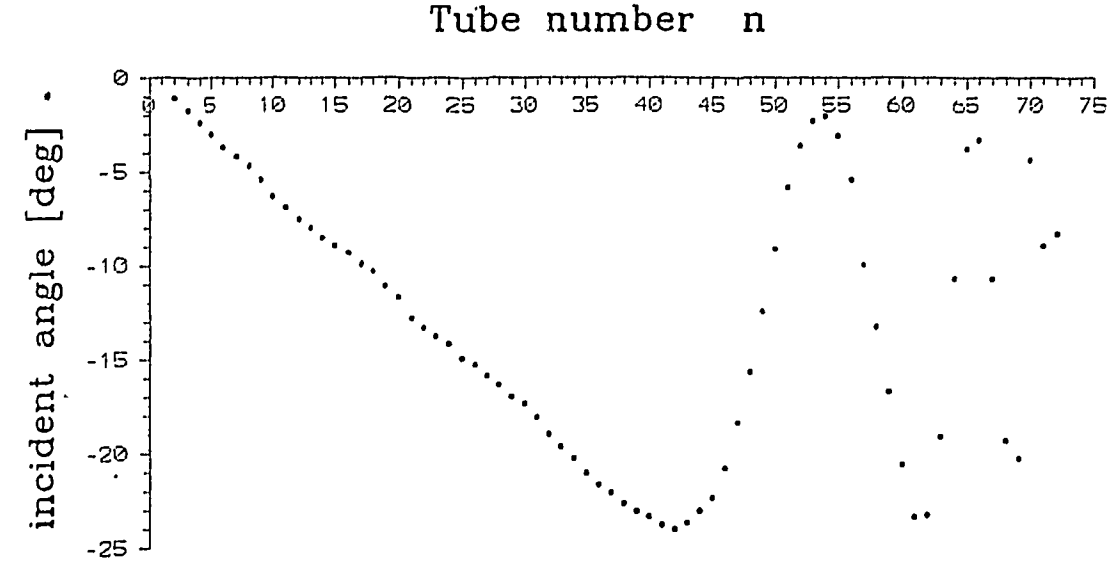

Figure 10: The dependence of particle incident angle c on tube number n

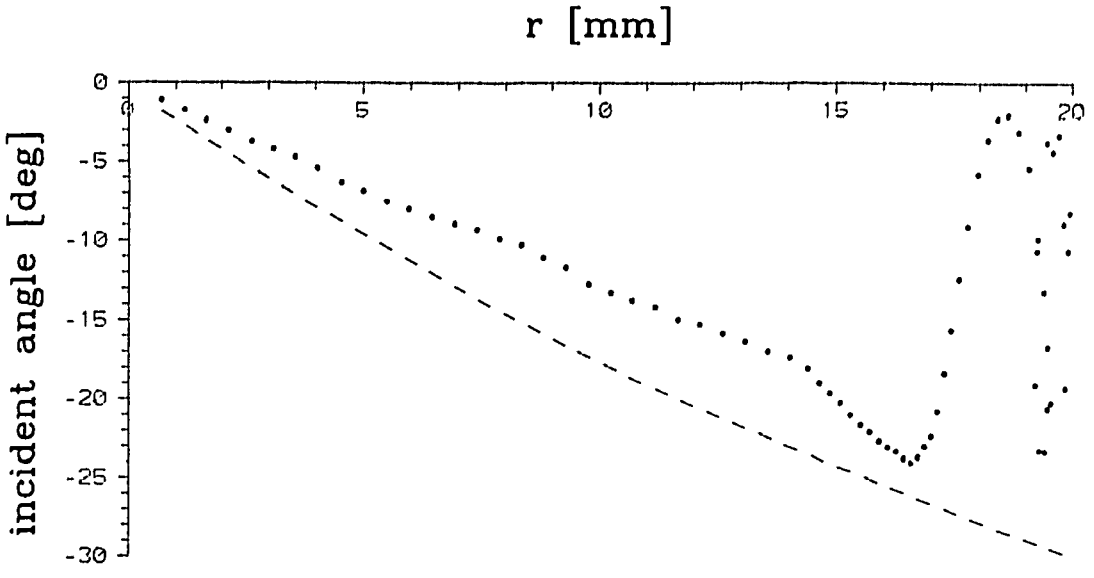

Figure 11: The dependence of the incident angle ϵ on beam radius r

numerical simulation of cylindrical diode (solid line), theoretical calculation of planar diode (dashed line)

in narrow periphery beam part, where the trajectories mixing occurred. The angular velocity spread of periphery particles is undesirable and might be dangerous for the excitation of two stream instability by REB in plasma column.

4 SUMMARY

The generation of REB by planar and cylindrical diode immersed in strong magnetic field has been performed. The homogeneity and particle angular velocity spread of generated beam have been investigated. The theoretical estimation done for planar diode has been compared with numerical simulation performed for cylindrical diode. In both cases the good coincidence for diode current density has been achieved. In the case of cylindrical diode the current density falls down on the beam periphery. The total diode current approaches to the value $I_b \simeq 76\ kA$, the theoretical predicted value doesn't differ from numerical one.

The internal magnetic field in central beam region monotonously grows up with the beam radius. For cylindrical diode the maximum value of internal azimuthal magnetic field has been achieved on the beam periphery. Then the magnetic field falls down inversely proportional to the radius.

The dependence of the angle between the particle trajectories and the direction of external longitudinal magnetic field has the same character for planar and cylindrical diode. The absolute values of incident deflection angle for planar diode are

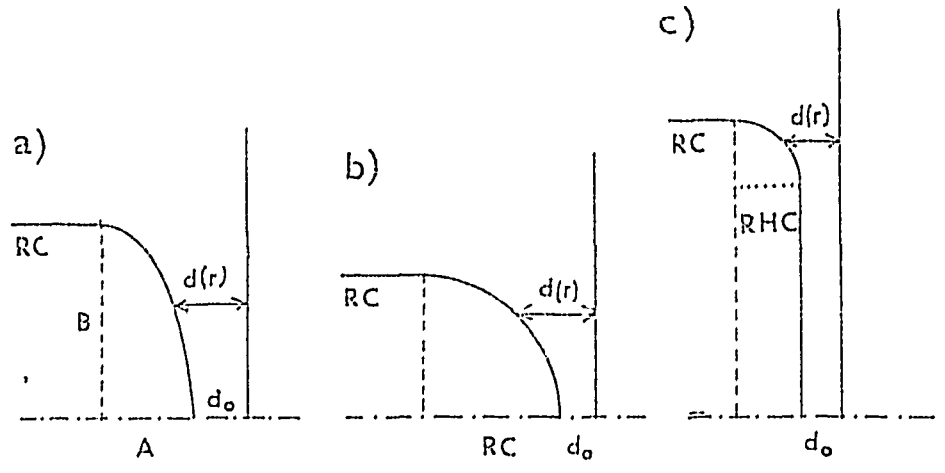

Figure 12: The projection of cathode cylindrical surfaces into r,z plane

a) - the ellipse, b) - the circle, c) - the line with circle

greater than for cylindrical diode, but the differences are $\lesssim$ 15 %. For cylindrical diode the chaos in particle incident angle has been detected in narrow periphery beam part. The incident angle changes chaotically from -2^0 to -25^0 in this region. The detected angular velocity spread of periphery beam particle may negatively influence the excitation of two stream instability in plasma column

The obtained results might be used for further optimization of high current foilless diodes

The work was supported in part by the Grant Agency of the Acad. Sci. of Czech Rep. under No: 14311

5 APPENDIX I

We determine the maximum value of the function $\frac{r}{d(r)}$, where $d(r)$ is the distance between cathode and anode. From practical reason is better to determine the minimum of the inverse function $\frac{d(r)}{r}$ than the maximum of original function, the result is same. The calculation will be done for various type of projections of cathode surface into r,z plane (see Fig. 12):

a) - the ellipse

The inverse function is

$$\frac{d(r)}{r} = \frac{d_0 + A(1 - \sqrt{1 - (\frac{r}{RC})^2})}{r}$$

where $B = RC$.

The derivative of the inverse function is

$$\frac{d}{dr}[\frac{d(r)}{r}] = -\frac{d_0 + A}{r^2} + \frac{A.RC}{r^2\sqrt{RC^2 - r^2}}$$

The point where the minimum (maximum) of inverse (original) function lies $r^* = \pm RC\sqrt{1 - (\frac{A}{d_0+A})^2}$, only + sign has the physical meaning.

The maximum of the original function $\frac{r}{d(r)}$ is

$$\max_{r^*}[\frac{r}{d(r)}] = \frac{RC}{\sqrt{d_0^2 + 2d_0.A}}$$

for $d_0 = A$ follows $r^* = \frac{\sqrt{3}}{2}RC$ and for $\max_{r^*}[\frac{r}{d(r)}] = \frac{RC}{\sqrt{3}d_0}$.

b) - the circle

From the above case introducing $A = B = RC$ we obtain for the point where the minimum (maximum) of inverse (original) function lies $r^* = RC\sqrt{1 - (\frac{RC}{d_0+RC})^2}$.

The maximum of the original function $\frac{r}{d(r)}$ is

$$\max_{r^*}[\frac{r}{d(r)}] = \frac{RC}{\sqrt{d_0^2 + 2d_0.RC}}$$

for $d_0 = RC$ follows $r^* = \frac{\sqrt{3}}{2}RC$ and for $\max_{r^*}[\frac{r}{d(r)}] = \frac{1}{\sqrt{3}}$.

c) - the line with circle

For $r \leq RC$ the inverse function is

$$\frac{d(r)}{r} = \frac{d_0}{r}$$

and for $r \geq RC$

$$\frac{d(r)}{r} = \frac{d_0 + RHC - \sqrt{RHC^2 - (r - RC)^2}}{r}$$

Let us suppose that $RC \gg 2d_0$ and $d_0 \simeq RHC$ (very common case), than for the point where the minimum (maximum) of inverse (original) function lies $r^* = RC + \frac{2d_0^2}{RC}$

The maximum of the original function $\frac{r}{d(r)}$ is

$$\max_{r^*}[\frac{r}{d(r)}] = \frac{RC^2 + 2d_0^2}{2d_0RC - d_0\sqrt{RC^2 - 4d_0^2}}$$

The other profiles (which coincide with the equipotential lines) are feasible.

References

[1] E.P. Kruglyakov I.V. Kandaurov and O.I. Meshkov. Foilless injection of reb into a dense plasma. In *The 9th Int. Conf. on High-Power Particle Beams*, page 1027, 1992.

[2] P. Šunka V. Piffl, M. Člupek and P. Vrba. Reb energy deposition in modified rebex experiment. In Jan Píchal, editor, *The 16 th Symposium on Plasma Physics and Technology*, pages 137–145. Czech Technical University, Institute of Plasma Physics, 1993.

[3] D.D Ruytov B.N. Breizman and G.V. Stupakov. The theory of high current diode with high aspect ratio. *Izvestia Vyshich Ucebnych Zavedenij*, (10) 7–26, 1979.

[4] P. Vrba. User's guide poisson2 (in czech). In *Report VZ 16/88*, pages 1 - 30. Institute of Plasma Physics, Acad. Sci. CR., 1988.

[5] P.Šunka P. Vrba and N.I. Gaponenko. Numerical simulation of ion beam generated in diode with anode plasma column. *Czechoslovak Journal of Physics*, 41(12) 1239–1247, 1991.

[6] V.I. Engelko P. Vrba, O.L. Komarov and Y.M. Saveljev. Influence of collector ions on operation of magnetically insulated diode. *Laser and Particle Beams*, 10(3) 531, 1992.

[7] P. Vrba and V. Piffl. The angular velocity spread of reb induced by magnetic field discontinuty. *Czechoslovak Journal of Physics*, 43(11) 1117–1128. 1993.